THE BELL SYSTEM TECHNICAL JOURNAL
Vol. 54, No. 2, February 1975
*Printed in U.S.A.*

# An Optical-Frequency Pulse-Position-Modulation Experiment

By W. S. HOLDEN

(Manuscript received April 3, 1974)

*This paper describes an optical-frequency pulse-position-modulation experiment using a GaAs luminescent diode as the source and either a PIN or an avalanche photodiode as the detector. The experimental system transmits an audio band from 300 Hz to 3.4 kHz at an 8-kb/s repetition rate. Timing synchronization between the transmitter and receiver has been accomplished by two methods: by transmitting a separate clock signal and by recovering the timing from the PPM signal itself. Data show, with each scheme, peak-signal-to-RMS-noise ratios of 70 dB can be achieved with the required average optical power at the receiver being −73 dBm with a PIN detector and −88 dBm with an avalanche detector.*

## I. INTRODUCTION

Recent advances in low-loss optical fibers,[1] in solid-state photodetectors,[2] and in optical-frequency (O.F.) power sources[3,4] have stimulated interest in O.F. communication systems for numerous applications. Pulse-position modulation (PPM) is particularly attractive for O.F. communications because the optical energy source can be operated at a low, message-independent, duty cycle to extend the lifetime of the device, and the technique affords a high noise immunity to the types of noise that dominate in a well-designed optical receiver. By employing a short pulse width and thereby expanding the bandwidth of the transmitted signal, the effect of detector leakage noise (dark current) and some forms of amplifier noise are reduced.

This paper describes an experiment performed to evaluate the performance that can be achieved in transmitting a single message channel by means of optical PPM.* Included are descriptions of the following:

* In an independent work (Ref. 5), a transmitter and receiver are described for an optical PPM system in which timing information was provided by a reference pulse in each time slot. The signal-to-noise ratio performance of the receiver was not given.

(*i*) The modulator that encodes the audio signal into a PPM signal.
(*ii*) The optical link using a GaAs LED as the source and either a PIN or an avalanche photodetector at the receiver.
(*iii*) The detection circuitry employing high-impedance front-end amplification techniques.[6,7]
(*iv*) The demodulator that transforms the PPM back to the original audio signal.
(*v*) The timing recovery scheme implemented using a phase-locked loop with the phase discriminator being the demodulator itself.
(*vi*) The results of experiments performed to measure the system performance.

## II. THE OVERALL SYSTEM

Figures 1a and 1b are block diagrams of the overall transmitter and receiver, respectively. Included are diagrams of the associated waveforms.

An audio signal, filtered to limit the transmitted bandwidth from 300 Hz to 3.4 kHz (3-dB points), is applied to a "sample-and-hold" circuit that transforms it into a staircase waveform having a step width of 125 $\mu$s. This staircase and an *inverted* 8-kHz sawtooth are applied to a comparator. The comparator output is high during the interval in which the sawtooth amplitude is greater than the staircase and low when the staircase amplitude exceeds that of the sawtooth. This results in pulse-width modulation (PWM) at an 8-kb/s repetition rate with the falling edge of each pulse varying in position within a time slot; this position relates directly to the audio signal amplitude. By adjusting the DC offset on the sawtooth, the trailing edge of the pulse is set to occur at the midpoint of the time slot when there is no audio input. This position corresponds to the zero reference.

Pulse-position modulation is obtained from PWM by producing a narrow pulse each time the comparator goes from a high to a low state. The timing components for the device were chosen to produce an output pulse width of the order of 0.5 $\mu$s. This results in a duty cycle of 0.4 percent, which is compatible with present state-of-the-art, large-optical-cavity, solid-state lasers.[8] (These lasers are capable of being operated with up to a 1-percent duty cycle.)

The PPM signal is amplified and applied to a GaAs light-emitting diode (LED) by means of a driver stage. The driver is capable of applying 500-mA pulses to an LED. During this experiment, however, the LED was driven by pulses having peak amplitudes between 200 and 300 mA.

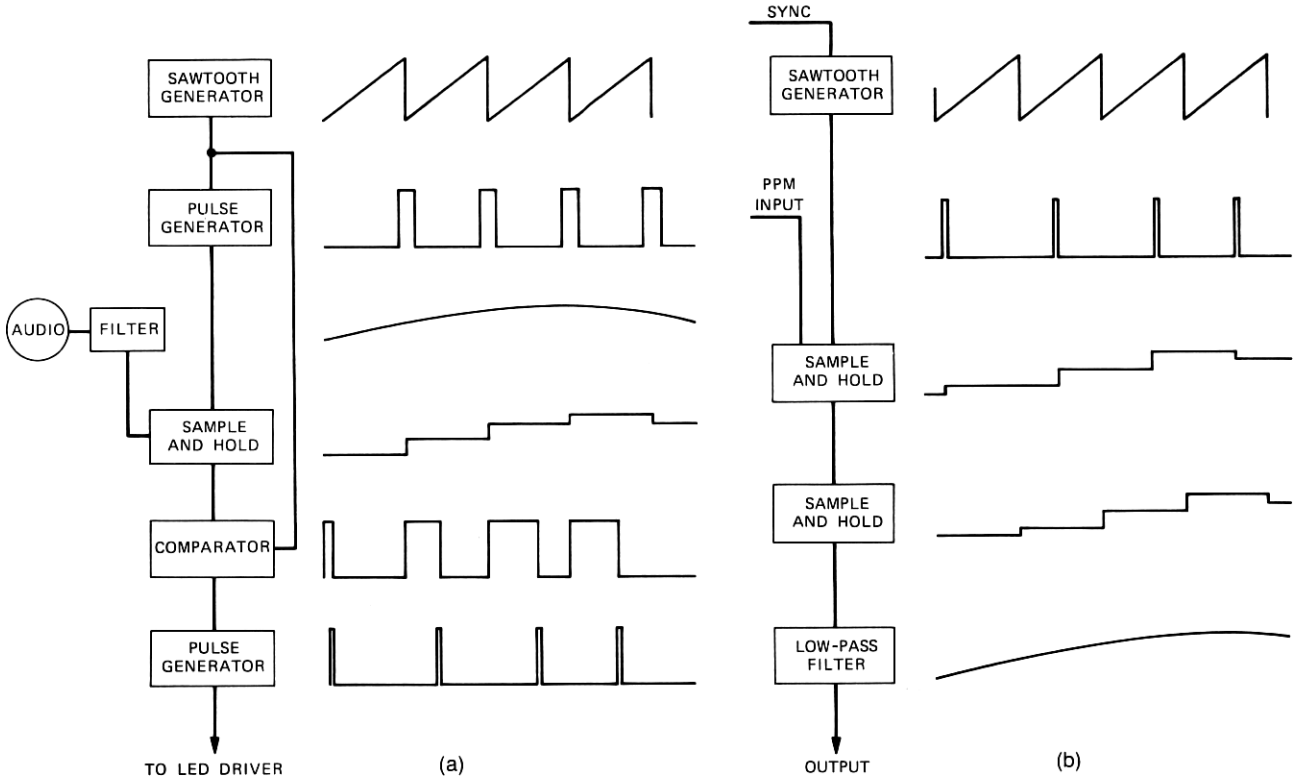


Fig. 1—(a) Block diagram and waveforms associated with the PPM transmitter. (b) Block diagram and waveforms associated with the PPM receiver.

In this experiment, the optical signal traverses an air path. Fiber loss is simulated by neutral density filters (providing large amounts of attenuation) and a pair of crossed polarizers (providing small but precise changes in attenuation). At the receiver, the signal is focused onto a photodetector, either a PIN or an avalanche device. The external quantum efficiency (amperes/watt) for each device has been measured. From this, by monitoring the average current through the device, the received average optical power may be obtained.

The detected signal, before demodulation, is processed by the following three stages:

(*i*) High-impedance front-end amplification—This approach is similar to that taken by J. E. Goell in his 6.3-Mb/s repeater research.[7] Figure 2 is a block diagram of the three-stage amplifier used. The first stage provides a high impedance for the photodetector, the second provides variable gain, and the third, a source follower, is provided to decouple the input amplifier from subsequent circuits.

(*ii*) Equalization—To compensate for the distortion introduced by the long input time constant, the circuit of Fig. 3 is used. The equalizer, a series capacitor and a resistance shunted to ground, is wired between two video amplifiers.

(*iii*) Filter—This stage, a two-section, low-pass Butterworth filter, limits the bandwidth of the signal pulse and noise. Two emitter-follower stages supply the proper impedances at the input and output (Fig. 4).

The PPM signal from the detection circuitry described above is applied to one input of a comparator. The other comparator input, which determines the threshold of the device, is connected to a variable DC source. This threshold was set with the received optical signal at the minimum value for which the demodulated audio output, when viewed on an oscilloscope, showed no distortion or noise. This method is justified because, for signal levels slightly higher than this value, the signal-independent noise is dominant.

The demodulator consists, basically, of two sample-and-hold circuits and a low-pass filter. The first sample-and-hold circuit is triggered by the PPM signal and samples a sawtooth wave. The output is a staircase with the following properties:

(*i*) The amplitude of each step varies as a function of the position of the received pulse in the time slot.

(*ii*) The step width varies according to the PPM signal.

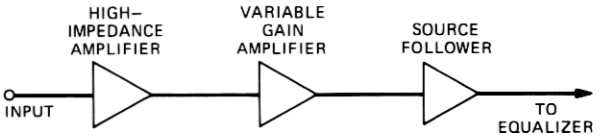


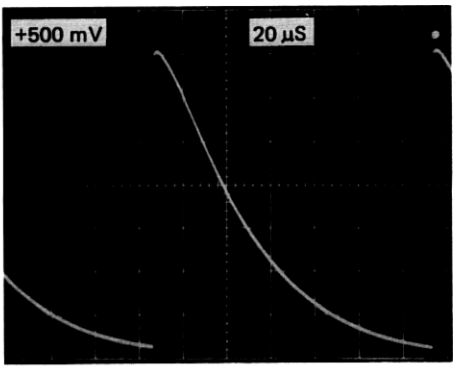


OUTPUT WAVEFORM

Fig. 2—High-impedance front-end amplifiers and output waveform.

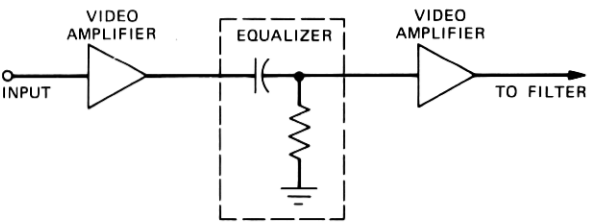


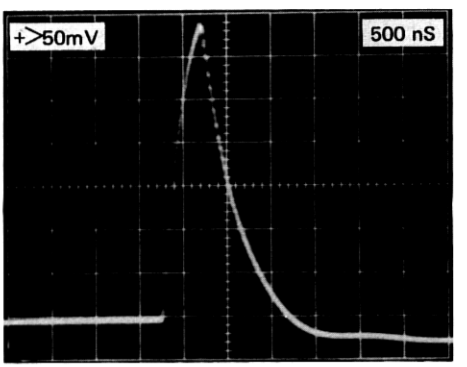


OUTPUT WAVEFORM

Fig. 3—Equalizer stage and output waveform.

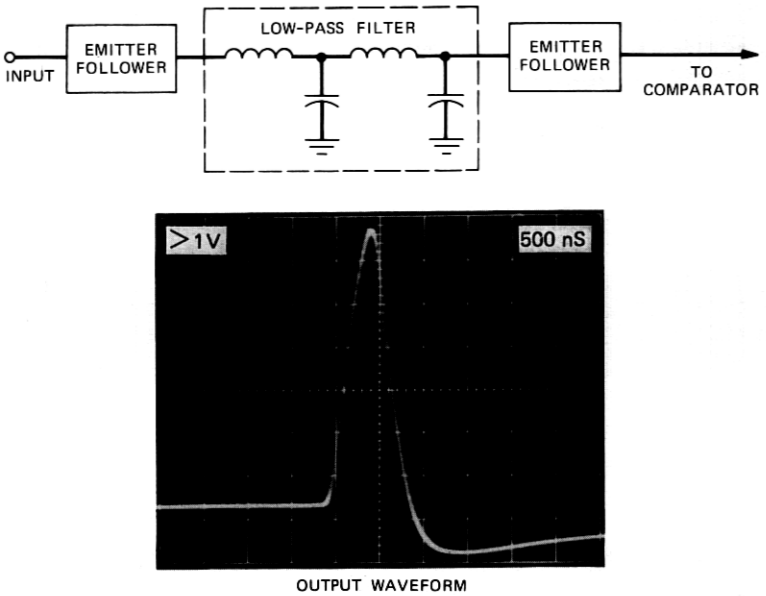


Fig. 4—Low-pass filter stage and output waveform.

Constant step width is achieved by using a second sample-and-hold circuit triggered by a repetitive 8-kb/s pulse train.

Filtering this staircase waveform removes the high-frequency components introduced by the sampling circuits and yields the original audio signal.

The timing recovery scheme incorporated in the receiver is described in the appendix.

## III. EXPERIMENTAL PROCEDURE AND RESULTS

This section describes the experiments performed to measure the channel's performance.

For the noise measurements, additional filtering was provided to suppress the third harmonic of the 60-Hz supply voltage, the high frequencies introduced in sampling (in the modulator and demodulator), and out-of-band thermal noise. The filter employed, a Rockland Model 1100, was set for a Butterworth high-pass response and a Bessel low-pass response. The passband (300 Hz to 3.4 kHz) has a ripple of $\pm 0.5$ dB and a 24-dB/octave rolloff.

A RMS voltmeter was used to measure peak-signal-to-RMS noise ratios* at the receiver output. The baseband signal level was measured

* This ratio will be referred to as SNR.

and converted to its corresponding peak value for the largest possible signal pulse excursion transmitted through the channel. The RMS noise was recorded directly, being measured with no audio signal applied. The optical pulse in all cases has a 20-ns rise time and a 3-dB width of 500 ns.

### *3.1 PIN detector*

Figure 5 shows the SNR's in dB plotted as a function of received average optical power. Four bandwidths were implemented by the low-pass filter in the detection circuitry which sets the bandwidth for the detected signal pulse and noise; the 3-dB widths are 5.5 MHz, 1 MHz, 600 kHz, and 200 kHz. These curves exhibit three regions: rapid increase, gradual increase, and no increase in SNR with increasing optical power.

For optical signal levels of the rapidly increasing region, the output noise is primarily due to spurious threshold crossings caused by front-end amplifier thermal noise. This noise may also add to the signal pulse such that it will not exceed the predetermined level.

In the gradually increasing region, the predominant degradation is due to time jitter on the transmitted pulse, originating in the transmitter. The front-end noise also leads to an uncertainty in determina-

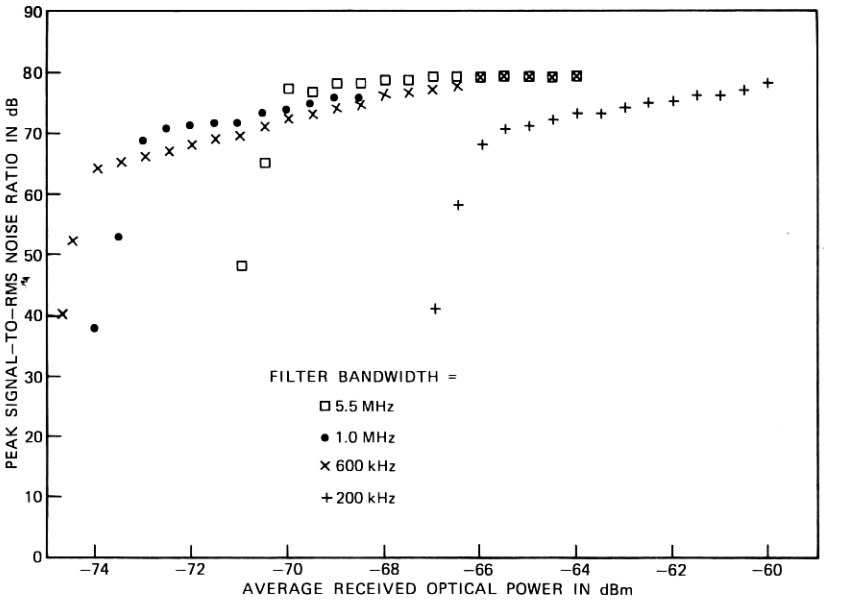


Fig. 5—Peak signal to RMS noise ratio in dB plotted as a function of average received optical power in dBm using a PIN detector.

tion of the time of a threshold crossing. With increasing power, the effect of this front-end jitter is reduced.

For optical signal levels greater than −66 dBm and for filter bandwidths of 5.5 MHz, 1 MHz, and 600 kHz, the noise resulting from the amplifiers and sampling circuits in the transmitter and receiver limits the performance. This effect occurs at −59 dBm for the 200-kHz filter. Increasing the received optical power does not improve the SNR in this region.

As the filter bandwidth decreases from 5.5 MHz to 600 kHz, both the noise and signal decrease. It can be shown that, with the high-impedance front-end, the noise (which is dominated by the FET-series noise source) decreases faster.[9] Thus, the power required to prevent threshold violations decreases with decreasing bandwidth. This effect is evident in Fig. 5. However, if the filter is too narrow, leakage noise will begin to dominate the FET-series noise source, and the required power will increase with decreasing filter width. This occurs in going from the 600-kHz to the 200-kHz filter. In the gradual increase region, increasing the filter width increases the noise voltage more slowly than the pulse slope for all cases. Therefore, increasing the bandwidth increases the SNR at a specified power level until threshold violations become significant.

### *3.2 Avalanche gain*

For this stage of the experiment, the PIN detector was replaced with a Texas Instrument TIXL 56 avalanche detector. The filter bandwidth in all cases was set to 1 MHz.

Figure 6 shows SNR plotted as a function of average received optical power for avalanche gains at 1, 10, 50, 65, and 80. (The accuracy of the measured SNR's is of the order of ±1.5 dB.) We see from this that, by increasing the avalanche gain from 1 to ≈ 60, less optical signal power is required to achieve a given SNR. The optimum gain for this device is ≈ 60. For avalanche gains larger than ≈ 60, the excess avalanche noise, rather than thermal noise, becomes dominant and, since this noise increases faster than the signal as avalanche gain is increased, more signal power is required to achieve a given SNR. Data for an avalanche gain of 80 illustrate this point, as it requires a received power of −83.5 dBm to achieve a 75-dB SNR. However, a 75-dB SNR may be achieved at a level of −85.5 dBm with a gain of 65.

With the avalanche detector biased for optimum gain, ≈15-dB more loss may be tolerated between transmitter and receiver than in the case with unity gain.

The data for Figs. 5 and 6 were recorded for the following two methods employed to synchronize the receiver: by transmitting a

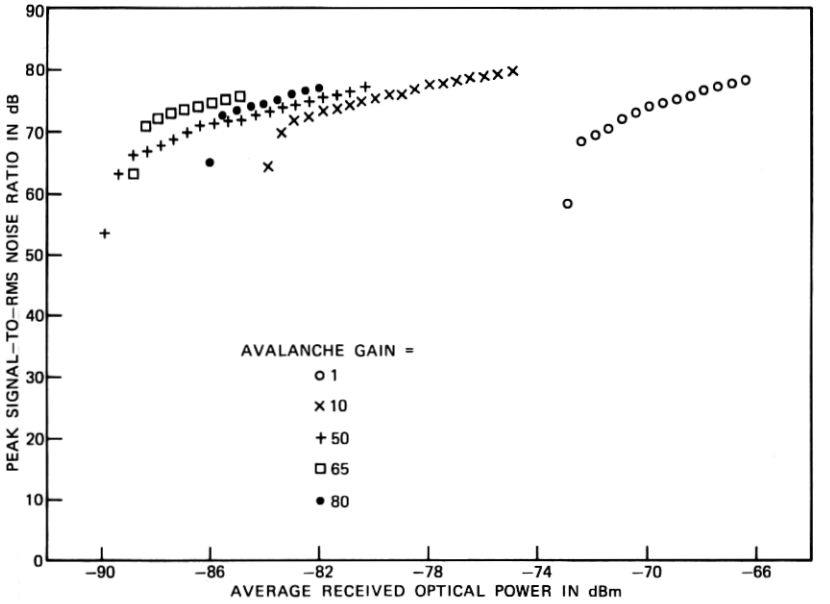


Fig. 6—Peak signal to RMS noise ratio in dB plotted as a function of average received optical power in dBm using an avalanche detector.

separate clock signal and by recovering the timing from the PPM signal itself. (This is discussed in detail in the appendix.) Differences in performance of the order of ±0.5 dB were observed; for this reason, it is concluded that the timing recovery circuit functioned properly over the range of power levels used in the experiments.

### *3.3 Distortion*

Distortion present on the output signal is shown in Figs. 7a, 7b, and 7c. The photographs show the output for SNR's at 75 dB, 77 dB, and 79 dB, respectively. Because the RMS noise is constant, the SNR here is determined by the signal amplitude. This distortion is introduced by the sampling circuits and amplifiers. It is not a basic limitation of the system. The degree of distortion was investigated using a spectrum analyzer to measure the relative amplitudes of the fundamental, second-harmonic, and third-harmonic components for different audio signal levels. Figure 7d shows the relative difference between the fundamental and second harmonic and between the fundamental and third harmonic plotted as a function of signal power. With full modulation (Fig. 7c), the second-harmonic distortion is 10 dB below the fundamental.

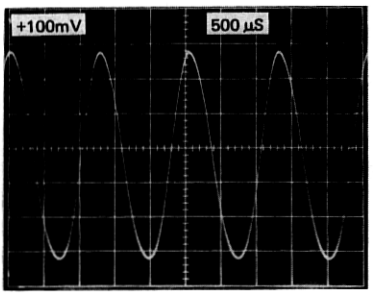


(a)

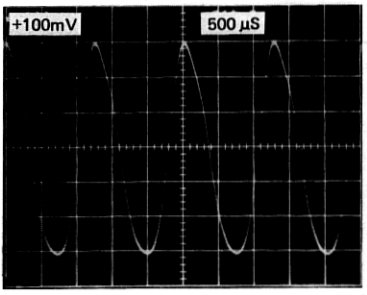


(b)

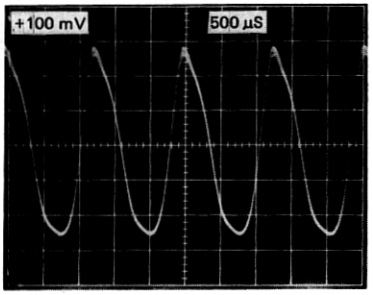


(c)

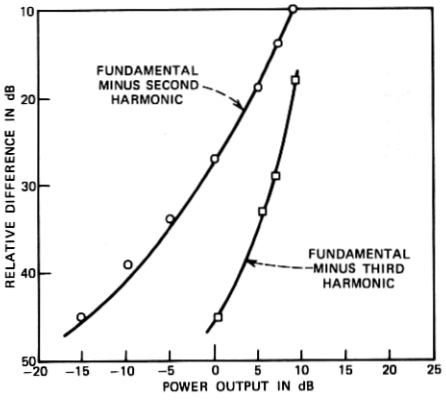


(d)

Fig. 7—Distortion on the output signal for SNR's of (a) 75 dB, (b) 77 dB, and (c) 79 dB. (d) Relative difference between the fundamental and second harmonic and the fundamental and third harmonic in dB plotted as a function of power out in dB.

## IV. CONCLUSIONS

An optical PPM communication experiment has been described. The receiver is capable of recovering timing synchronization from the transmitted PPM signal itself. Peak-signal-to-RMS noise ratios greater than 70 dB (the objective of the experiment) have been achieved. By using a PIN detector and a 1-MHz filter, this objective can be achieved at an average received optical power level of −73 dBm. With full modulation, the second-harmonic distortion is 10 dB below the fundamental. Since existing LED's can couple −10 dBm of average optical signal power into an optical fiber, the allowable attenuation would be $\approx$ 60 dB, which allows a range of 15 km for fibers having 4-dB/km loss. However, with a large-optical-cavity laser as the source, we can contemplate that as much as +20 dBm might be injected into a fiber; this would increase the tolerable attenuation to $\approx$ 90 dB (corresponding to a range of $\approx$ 22 km). Data show that an additional improvement

of 15 dB may be obtained by using avalanche gain in the receiver. A PPM system of this nature would be able to tolerate $\approx$ 105 dB of fiber loss between transmitter and receiver. This corresponds to $\approx$ 26 km of fiber, which makes this system very attractive.


## V. ACKNOWLEDGMENT

The author is grateful to C. A. Burrus for providing the LED, to Rudy Drexler and Paul Fleischer for the active filter design, and to J. E. Goell for his advice and assistance in fabrication of the system.


## APPENDIX

A PPM system requires timing synchronization between transmitter and receiver clocks.[10] Two methods have been employed to accomplish synchronization. The first is to simply carry a timing signal from the transmitter to the receiver by a coaxial cable. The second method, which is described in this section, is a scheme that recovers the timing from the transmitted PPM signal itself.

The sawtooth oscillators in the transmitter and receiver have been designed to free run at approximately the same frequency; however, bias-voltage fluctuations and temperature changes may cause one to drift with respect to the other.

A change in relative phase results in a DC level shift at the output of the first sample-and-hold circuit in the demodulator. This DC level is defined as the error signal. To compensate for this frequency drift, the error signal is applied to a voltage-controlled oscillator (VCO) in such a manner as to change the oscillator frequency in opposition to the initial frequency drift. In essence, the demodulator acts as a phase discriminator in a phase-locked loop.

The VCO and associated circuitry, shown in Fig. 8, are used to complete the loop when connected between the first sample-and-hold output and the sawtooth-trigger input. The sampled output contains two components, an audio staircase and the error signal. The error signal is amplified by the operational amplifier, while the audio is suppressed

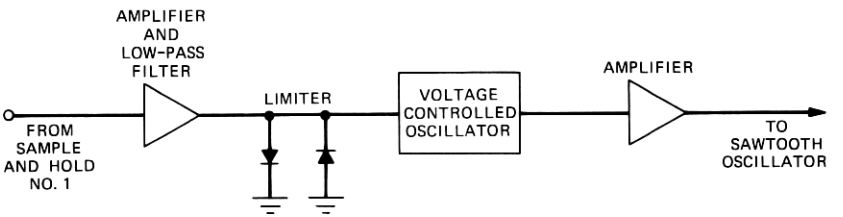


Fig. 8—Voltage-controlled oscillator and associated circuitry.

by the feedback capacitor. The differential input sets the loop reference. Two diodes connected back to back at the operational amplifier output serve to limit the frequency range over which the vco can be varied. The error signal is further amplified and applied across the vco. The final stage amplifies the vco output to a sufficient level to trigger the sawtooth generator.

## REFERENCES


1. D. B. Keck, R. D. Maurer, and P. C. Shultz, "On the Ultimate Lower Limit of Attenuation in Glass Optical Waveguides," Appl. Phys. Let., *22*, No. 7 (April 1973), pp. 307–309.
2. H. Melchior, M. B. Fisher, F. R. Arams, "Photodetectors for Optical Communication Systems," Proc. IEEE, *48*, No. 10 (October 1970), pp. 1466–1486.
3. C. A. Burrus and B. I. Miller, "Small-Area, Double Heterostructure Aluminum-Gallium-Arsenide Electroluminescent Diode Sources for Optical-Fiber Transmission Lines," Opt. Commun., *4*, No. 4 (December 1971), pp. 307–309.
4. B. I. Miller, J. E. Ripper, J. C. Dyment, E. Pinkas, and M. B. Panish, "Semiconductor Lasers Operating Continuously in the 'Visible' at Room Temperature," Appl. Phys. Lett., *18*, No. 9 (May 1, 1971), pp. 403–405.
5. B. S. S. Rao, A. Subrahmanyam, and Prem Swarup, "A Technique of Modulating Pulsed Semiconductor Lasers," IEEE Trans. Commun., *COM-21*, No. 4 (April 1973), pp. 284–289.
6. S. D. Personick, "Applications for Quantum Amplifiers in Simple Digital Optical Communication Systems," B.S.T.J., *52*, No. 1 (January 1973), pp. 117–133.
7. J. E. Goell, "An Optical Repeater With High-Impedance Input Amplifier," B.S.T.J., *53*, No. 4 (April 1974), pp. 629–643.
8. H. Kressel, H. F. Lockwood, and F. Z. Hawrylo, "Large Optical Cavity (AlGa) As-GaAs Herojunction Laser Diode: Threshold and Efficiency," J. Appl. Phys., *43* (February 1972), pp. 561–567.
9. S. D. Personick, "Receiver Design for Digital Fiber Optic Communication Systems, I," B.S.T.J., *52*, No. 6 (July–August 1973), pp. 843–874.
10. R. Gagilardi, "Synchronization Using Pulsed Edge Tracking in Optical PPM Communication System," Interim Technical Report (University of Southern California), September 1972.